Effect of milling time variation on TiTaVWCr HEA powder as nuclear material on microstructure and mechanical properties by a mechanical alloying method

by Teknologi Industri

Submission date: 05-Oct-2023 09:00PM (UTC-0400)
Submission ID: 2141154795
File name: CONSER_2022_PaperID_8998.docx (2.48M)
Word count: 3342
Character count: 18688

Effect of milling time variation on TiTaVWCr HEA powder as nuclear material on microstructure and mechanical properties by a mechanical alloying method

Sutrisna[1*], Angger Bagus Prasetiyo [2], Ratna Kartikasari[3], Ihwanul Aziz[4,]

[1*,2,3,]Department of Mechanical Engineering, Institut Teknologi Nasional Yogyakarta, 55281, Indonesia
[4]Research Center for Accelerator Technology, National Research and Innovation Agency, Indonesia

Corresponding author: sutrisna@itny.ac.id

Abstract

TiTaVWCr HEA alloy is a refractory material that is often used as nuclear material. This research uses powder material and milling using the mechanical alloy method. This research aimed to determine the microstructure and mechanical properties of the TiTaVWCr HEA alloy milling process for 4 h, 8 h, 16 h, and 24 h. Tests were carried out using XRD spectra and Secondary Electron Microstructure-Energy Dispersive Spectroscopy (SEM-EDS) to determine the characteristics of the material and its microstructure. The results showed that the HEA model with low milling (4 h and 8 h) microstructure distribution was not uniform, and there was agglomeration in certain areas. After milling was increased to 16 hours, the distribution of elements became uniform, but oxides appeared on Ti became in the formation of Ti-O. The hardness value shows that the longer the milling time, the higher the hardness. This phenomenon is related to the increase in grain dimension, and dislocation density.

Keywords: TiTaVWCr HEA, mechanical alloy, nuclear material, milling variation.

1. INTRODUCTION

High entropy alloys (HEA) are alloys of materials with atomic concentrations of 5% to 35% and consist of a minimum of five elements in molar ratios or near [1]. HEA is one of the most promising structural materials in current developments for various industrial, aerospace, automotive, and nuclear energy applications.[2][3]. In addition, HEA exhibits wonderful properties such as having high strength, high hardness value, good wear, and oxidation, and besides that, it is also resistant to corrosion, has high thermal stability, and has highly reputable mechanical properties [4][5]. Mixing HEA elements is a concept in the design of multi-component systems, and this concept will accelerate the development of new system alloys [6]. There are several techniques used in HEA fabrication, namely casting, arc-melting, sputtering, laser cladding, and mechanical alloying [7][8][9]. The melting temperature of HEA requires a very high temperature, hence it is made by melting and vacuum arc casting methods. Furthermore, the heat treatment process forms a homogeneous microstructure.

Recently, a mechanical alloying method has been developed for HEA production [10][11][12]. In this method, it is hoped that a smoother and more homogeneous mixture will be obtained.[13][14][15]. In addition, the mechanical alloying method can also combine and mix materials that have a high melting point with a low melting point [16][17]. Previous studies have reported by Owais A et al [18] that nuclear fusion devices such as WTaTiVCr at high temperatures and having a high melting point exhibit high mechanical properties. In addition, this type of HEA has recently been investigated such as TixWTaVCr [19], MoNbCrVTi [20], NbMoTaWVCr [21], and Wx(TaTiVCr)1-x [22]. Their results showed that the HEA had high strength and hardness and a BCC crystal structure. Likewise in the TiTaVWCr alloy, the BCC matrix occurs because of the Cr element which encourages the formation of the Laves phase. This happens because the element Cr has the smallest radius [23]. At high temperatures, the refractory HEA microstructure

can affect the mechanical properties that it can increase strength, while at room temperature, it decreases.[24]

In this study, the materials used for the HEA refractory alloy were powder elements Ti, Ta, V, W, and Cr using the mechanical alloy method and thoroughly characterized. This study aims to study the effect of variations in milling time 4 h, 8 h, 16 h, and 24 h on the mechanical properties and microstructure after sintering at 1450°C.

2. METHODOLOGY

In this study, a powder material consisting of Ti, Ta, V, W, and Cr elements was used. These elements have particle sizes between 1 - 50 microns and purity above 99.5%. The chemical composition is the same for all elements. The method used in this research is to mix the elements first with the same percentage. After these elements were mixed, they were milled using a mechanical alloy method for 4 h, 8 h, 16 h, and 24 h. The milling process uses a planetary ball mill machine with a rotation speed of 300 rpm and the ratio between balls and powders is 10:1. During the milling process to prevent agglomeration, stearic acid was given as a process control agent.

Furthermore, the powder that has been milled is compacted with a pressure of 5 tons within 5 seconds to become a green compact. Then the compacted green compact was sintered at 1450°C and held for 1 hour. The XRD spectrum test was used to characterize the phase of the powder, while SEM-EDS was used to determine the microstructure and composition. Furthermore, the Vickers method was used to measure the hardness value using a 1 kg load held for 15 seconds, while the Archimedes method was used to determine the relative density.

3. RESULTS AND DISCUSSION

3.2.1. Characterization of Powders

Figure 1 shows the change in characteristics of powder using XRD spectrum analysis on mixed powders between Ta, Ti, V, W, and Cr after milling for 4 h, 8 h, 16 h, and 24 h. The un-milled powder showed very strong peak detection on some of these elements, in this case, the W element had the highest peak. This is because element W has the highest atomic mass compared to the other elements in this alloy[25]. In addition to showing strong peak reflections from these elements, there are also elements whose peaks overlap between Ta and Ti. This happens because the two elements have atomic radii that are close together[26].

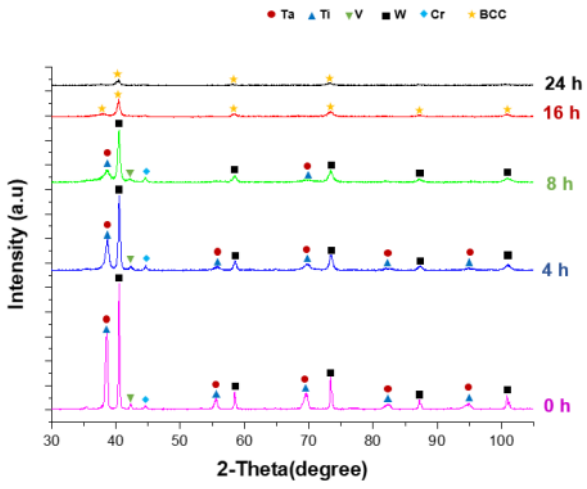

Figure 1. XRD spectra results of TiTaVWCr powder

After the milling time was increased from 4 h to 24 h there was a broadening of the peaks and the intensity decreased. This indicates that the milling process causes a decrease in crystal size. In addition, grain refinement and the occurrence of lattice strain are due to the grinding process. [27]. At the end of milling (24 h), BCC single-phase alloy powder structure was formed. [28], also due to the high-impact energy of the grinding medium and the long milling duration [29].

3.3. Microstructural Characterization

3.3.1. Microstructure Analysis

Microstructure of the TiTaVWCr equiatomic alloy with variations in grinding time for 4 h, 8 h, 16 h, and 24 h using the mechanical alloying method. The distribution of the structure is shown in Figure 2. At 4 hours of milling, the distribution of the structure was unequal in the HEA matrix; there was an agglomeration of Ti elements in certain areas. This shows that the milling is not complete and that diffusion occurs between the constituent elements. In addition, the solid solution has not been completely formed. The same thing happened to milling for 8 hours, as shown in Figures 2. a and 2. b, following the XRD test in Figure 1. After milling was increased to 16 hours. The distribution of the elements begins to be uniform, and a solid solution has occurred. However, element W still dominates the distribution and has a particle size of about 10 μm there are still significant differences in particle size. Increased milling time leads to even element distribution and smaller grains, and oxygen contamination. This is due to the grinding medium during the mechanical alloying process. [30]. In the final stage of milling, there is an even distribution of the oxide in the matrix. (Figure 2.d). In addition to the oxide dispersion, there is also elemental shrinkage and grain size refinement. As a result, the oxide particles that are produced when a Ti-rich precipitate is present form a core-shell, which reduces particle size and raises density. [31].

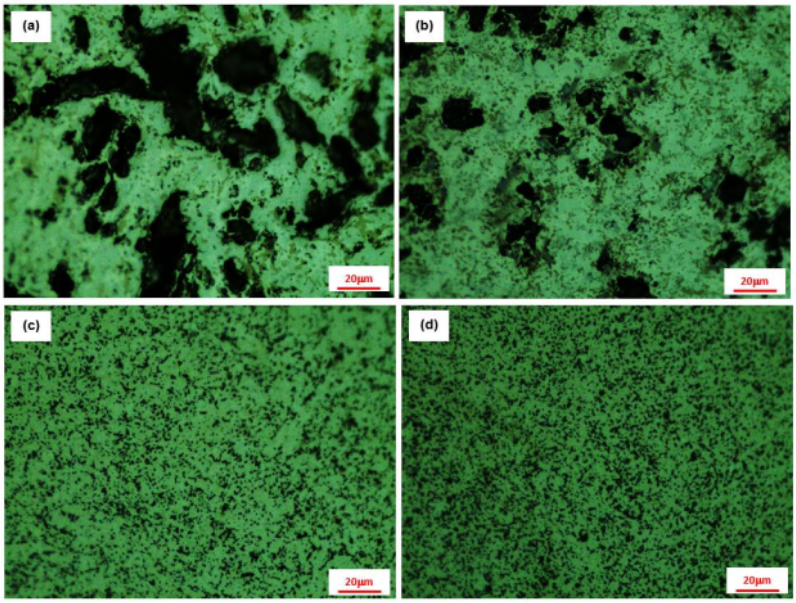

Figure 2. Results of optical microstructure with grinding time variation: (a). 4 h, (b). 8 h, (c). 16 h and (d). 24 h

3.3.2. EDS point Analysis

Figure 3 shows the EDS points of TiTaVWCr with variations in grinding time of 4 h, 8 h, 16 h, and 24 h. Milling for 4 h showed that the distribution of elements was incomplete that the distribution of elements

was unequal and that some elements agglomerated in certain areas. Point 1 shows the TiTaVWCr HEA matrix with dominant tungsten other than Cr and Vanadium with a gray color, and from the milling and sintering process, there is still agglomeration in certain areas. High concentrations of Ti and O were also found at point 2 in Figure 2.a. This shows that point 2 means that the oxide is rich-Ti, it also contains a small amount of element V. Furthermore, point 3 shows that Ti-oxide and elements V and Ta also appear, as well as what happened at milling of 8 h (Figure 3. b).

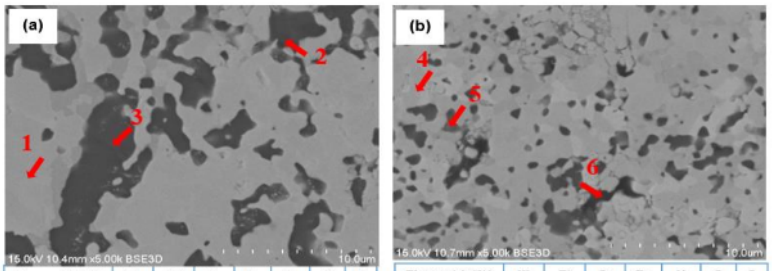

Element (at%)	W	Ti	Cr	Ta	V	O	C
1	54.87	-	19,85	-	25.28	-	-
2	-	28.58	-	-	7.10	64.32	-
3	-	32.69	-	0.74	10.04	56.69	-

Element (at%)	W	Ti	Cr	Ta	V	O	C
4	40.26	-	27.00	-	32.74	-	-
5	-	23.63	13.92	-	9.16	53.30	-
6	-	24.29	4.82	-	11.63	59.26	-

Element (at%)	W	Ti	Cr	Ta	V	O	C
7	52.85	-	24.23	-	22.91	-	-
8	5.90	29.58	4.96	3.86	9.15	46.55	-
9	1.67	28.19	5.88	-	8.10	56.16	-

Element (at%)	W	Ti	Cr	Ta	V	O	C
10	52.22	-	22.61	-	15.15	10.02	-
11	9.11	20.03	7.46	3.90	10.37	49.13	-
12	5.43	22.15	8.39	1.02	12.18	41.75	4.76

Figure 3. EDS images of the TiTaVWCr at grinding time of (a). 4 h, (b). 8 h, (c). 16 h and (d). 24 h

The presence of other elements appearing in the 8 h milling process indicates that the process has not completed the formation of a complete solid solution. After the milling time was increased to 16 h, a solid solution began to occur, and the distribution of elements spread evenly. At the end of 24 h of milling (see Figure 3.d) that the distribution of the elements is equal and a solid solution is formed. The distribution of elements is even between the HEA matrix and the other elements. The presence of oxides in the microstructure facilitates the formation of Ti oxide. The high oxide content in Ti can cause unwanted phase deposition during the sintering process. The deposition of this phase causes microstructure segregation.[17].

3.3.3. EDS Mapping Analysis

The results of mapping the TaTiVWCr alloy at a milling time of 24 h are shown in Figure 4. This was done to determine the composition of each element. In this figure, the distribution of each element is clearly visible. On the element Ti, the oxide is also clearly visible. This indicates that the Ti-rich oxide can be easily formed by mechanical alloys with long milling times and high-temperature sintering[32][33]. In addition, the uniform distribution of elements in HEA materials can be correlated with single-phase BCC solid solutions.

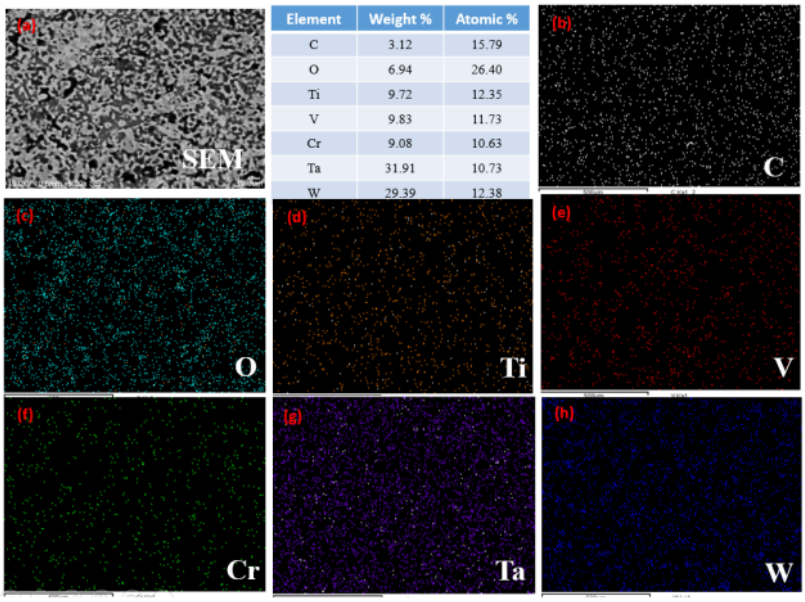

Figure 4. EDS mapping analysis of the TiTaVWCr after milling 24 h

3.3.4. Hardness Analysis.

Figure 5 shows the value of hardness that occurs during the milling process. It can be seen in the figure, that the longer the milling time, the higher the hardness value. At the beginning of milling (4 h), the hardness value was 432 HV. Furthermore, the milling time was increased to 8 h, there was a change in the hardness value that increased but was not significant (approximately 13%). This is correlated with the observation of the microstructure in Figure 2, that the distribution of the elements is not equally distributed, and there is no complete solid solution. After the milling time was increased to 16 h, there was a very significant increase in the hardness value (about 58%). This increase in hardness value is caused by the composition of the elements that have been equally distributed and a solid solution formation. At the end of milling for 24 h, the hardness value also increased to 1306 HV, apart from the uniform elements distribution and the solid solution formation, oxides and carbon also appear as a result of the sintering process at high temperatures (1450°). As for the sintering process, in addition to identifying an increase in the hardness value, there is also an improvement in grain size and an increase in dislocation density and strain energy.

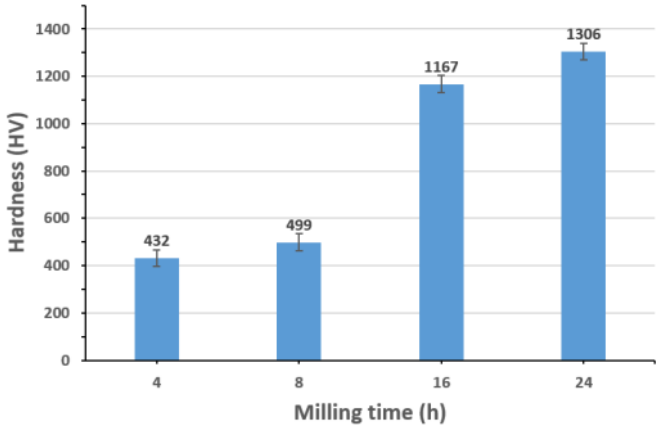

Figure 5. Vickers hardness value of the TiTaVWCr

The value of the relative density of TiTaVWCr is based on variations in milling time, the longer the milling time causes the density to be higher, as shown in Figure 6. Archimedes method was used in this measurement. At 4 h milling has a relative density of 83.75 gr/cm^3; after the milling time is increased to 8 h, there is no significant change. This happens because, during the 4 h and 8 h milling process, the results are not perfect; there is still agglomeration in certain areas in the TiTaVWCr HEA alloy, as shown in Figure 2 (microstructure). Furthermore, after the milling was raised again until the end of milling (24 h), the relative density was very high (98.38 gr/cm^3). It is closely related to the previous test (Figure 2. c – d and Figure 4), that after milling for 24 h a solid solution occurs.

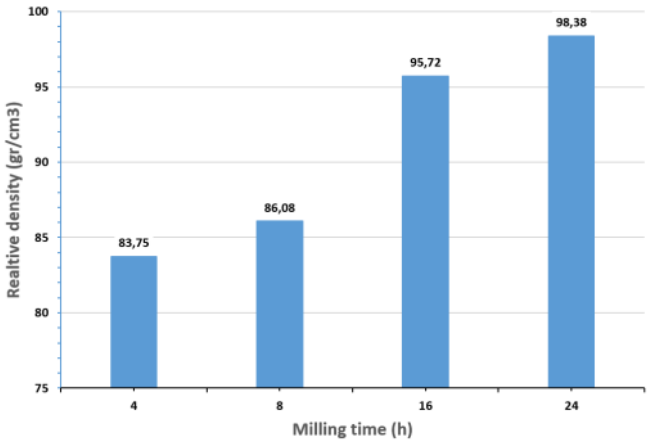

Figure 6. Relative density of the TiTaVWCr

4. CONCLUSIONS

Research has been carried out with variations in grinding time for 4 h, 8 h, 16 h, and 24 h on TiTaVWCr HEA equiatomic. The findings indicated that the solid solution phase of BCC was completely formed after 24 h milling, which was clearly visible on the XRD spectra test. The distribution of microstructure was equally distributed after 16 h, and at 24 h of milling time, oxides appeared which facilitated the Ti-oxide formation. Phase deposition is formed due to the presence of high oxide content in Ti which causes the microstructure separation. Furthermore, the hardness value shows an increase with the length of milling time. This can be attributed to smaller grain size, dislocation density, and increased strain energy

ACKNOWLEDGEMENTS

The author expresses his deepest gratitude to Institut Teknologi Nasional Yogyakarta for funding research and International conference, and Laboratory at Research Center for Accelerator Technology National Research and Innovation Agency Yogyakarta Indonesia provides facilities for research.

REFERENCES

[1] J.W. Yeh, S.K. Chen, S.J. Lin, J.Y. Gan, T.S. Chin, T.T. Shun, C.H. Tsau, S.Y. Chang, Nanostructured high-entropy alloys with multiple principal elements: Novel alloy design concepts and outcomes, Adv. Eng. Mater. 6 (2004) 299-303+274. https://doi.org/10.1002/adem.200300567.

[2] C. Xiang, E. Han, Z.M. Zhang, H.M. Fu, J.Q. Wang, H.F. Zhang, G.D. Hu, Design of single-phase high-entropy alloys composed of low thermal neutron absorption cross-section elements for nuclear power plant application, Intermetallics. 104 (2019) 143–153.

https://doi.org/10.1016/j.intermet.2018.11.001.
[3] L.M. and A.R. V Geanta, I Voiculescu, R Stefanoiu, T Chereches, T Zecheru, Dynamic Impact Behaviour of High Entropy Alloys Used in the Military Domain, Mater. Sci. Eng. 374 (2018) 1–12. https://doi.org/10.1088/1757-899X/374/1/012041.
[4] L. Moravcikova-gouvea, I. Moravcik, L. Gouvea, V. Hornik, Z. Kovacova, M. Kitzmantel, Synergic strengthening by oxide and coherent precipitate dispersions in high- entropy alloy prepared by powder metallurgy, Scr. Mater. 157 (2018) 24–29. https://doi.org/10.1016/j.scriptamat.2018.07.034.
[5] O.N. Senkov, G.B. Wilks, J.M. Scott, D.B. Miracle, Mechanical properties of Nb25Mo25Ta25W25 and V20Nb20Mo20Ta20W20 refractory high entropy alloys, Intermetallics. 19 (2011) 698–706. https://doi.org/10.1016/j.intermet.2011.01.004.
[6] Y. Zhang, Y.J. Zhou, J.P. Lin, G.L. Chen, P.K. Liaw, Solid-solution phase formation rules for multi-component alloys, Adv. Eng. Mater. 10 (2008) 534–538. https://doi.org/10.1002/adem.200700240.
[7] S. Joo, H. Kato, M.J. Jang, J. Moon, E.B. Kim, S. Hong, H.S. Kim, Structure and properties of ultra fine-grained CoCrFeMnNi high- entropy alloys produced by mechanical alloying and spark plasma sintering, J. Alloys Compd. 698 (2017) 591–604. https://doi.org/10.1016/j.jallcom.2016.12.010.
[8] Z. Chen, W. Chen, B. Wu, X. Cao, L. Liu, Z. Fu, Effects of Co and Ti on microstructure and mechanical behavior of Al 0 . 75 FeNiCrCo high entropy alloy prepared by mechanical alloying and spark plasma sintering, Mater. Sci. Eng. A. (2015) 0–32. https://doi.org/10.1016/j.msea.2015.08.056.
[9] B. Ren, Z.X. Liu, L. Shi, B. Cai, M.X. Wang, Structure and properties of (AlCrMnMoNiZrB 0.1)N x coatings prepared by reactive DC sputtering, Appl. Surf. Sci. 257 (2011) 7172–7178. https://doi.org/10.1016/j.apsusc.2011.03.083.
[10] C. Suryanarayana, N. Al-Aqeeli, Mechanically alloyed nanocomposites, Prog. Mater. Sci. 58 (2013) 383–502. https://doi.org/10.1016/j.pmatsci.2012.10.001.
[11] M. Vaidya, A. Karati, A. Marshal, K.G. Pradeep, B.S. Murty, Phase evolution and stability of nanocrystalline CoCrFeNi and CoCrFeMnNi high entropy alloys, J. Alloys Compd. 770 (2019) 1004–1015. https://doi.org/10.1016/j.jallcom.2018.08.200.
[12] X. Shang, X. Wang, S. Chen, Effects of ball milling processing conditions and alloy components on the synthesis of Cu-Nb and Cu-Mo alloys, Materials (Basel). 12 (2019) 1–9. https://doi.org/10.3390/ma12081224.
[13] P. Wang, H. Cai, S. Zhou, L. Xu, Processing, microstructure and properties of Ni1.5CoCuFeCr0.5−xVxhigh entropy alloys with carbon introduced from process control agent, J. Alloys Compd. 695 (2017) 462–475. https://doi.org/10.1016/j.jallcom.2016.10.288.
[14] H. Materials, N. Deng, Z. Zhou, J. Li, Y. Wu, International Journal of Refractory Metals W – Cu composites with homogenous Cu – network structure prepared by spark plasma sintering using core – shell powders, 82 (2019) 310–316.
[15] I. Matuła, M. Zubko, G. Dercz, Role of Sn as a process control agent on mechanical alloying behavior of nanocrystalline titanium based powders, Materials (Basel). 13 (2020) 9–12. https://doi.org/10.3390/ma13092110.
[16] J. Tan, Z.J. Zhou, X.P. Zhu, S.Q. Guo, D.D. Qu, M.K. Lei, C.C. Ge, Evaluation of ultra-fine grained tungsten under transient high heat flux by high-intensity pulsed ion beam, Trans. Nonferrous Met. Soc. China (English Ed. 22 (2012) 1081–1085. https://doi.org/10.1016/S1003-6326(11)61286-7.
[17] M. Vaidya, A. Karati, A. Marshal, K.G. Pradeep, B.S. Murty, Phase evolution and stability of nanocrystalline CoCrFeNi and CoCrFeMnNi high entropy alloys, J. Alloys Compd. 770 (2019) 1004–1015. https://doi.org/10.1016/j.jallcom.2018.08.200.
[18] O.A. Waseem, H.J. Ryu, Tungsten-Based Composites for Nuclear Fusion Applications, Nucl. Mater. Perform. (2016). https://doi.org/10.5772/62434.
[19] O.A. Waseem, J. Lee, H.M. Lee, H.J. Ryu, The effect of Ti on the sintering and mechanical

properties of refractory high-entropy alloy TixWTaVCr fabricated via spark plasma sintering for fusion plasma-facing materials, Mater. Chem. Phys. 210 (2018) 87–94. https://doi.org/10.1016/j.matchemphys.2017.06.054.

[20] C. Xiang, E.H. Han, Z.M. Zhang, H.M. Fu, J.Q. Wang, H.F. Zhang, G.D. Hu, Design of single-phase high-entropy alloys composed of low thermal neutron absorption cross-section elements for nuclear power plant application, Intermetallics. 104 (2019) 143–153. https://doi.org/10.1016/j.intermet.2018.11.001.

[21] Y. Long, X. Liang, K. Su, H. Peng, X. Li, A fine-grained NbMoTaWVCr refractory high-entropy alloy with ultra-high strength: Microstructural evolution and mechanical properties, J. Alloys Compd. 780 (2019) 607–617. https://doi.org/10.1016/j.jallcom.2018.11.318.

[22] X.J. Yao, X.F. Shi, Y.P. Wang, G.Y. Gan, B.Y. Tang, The mechanical properties of high entropy (-like) alloy Wx(TaTiVCr)1-x via first-principles calculations, Fusion Eng. Des. 137 (2018) 35–42. https://doi.org/10.1016/j.fusengdes.2018.08.008.

[23] H. Materials, A.G. Hamidi, H. Arabi, J.V. Khaki, International Journal of Refractory Metals Sintering of a nano-crystalline tungsten heavy alloy powder, Int. J. Refract. Metals Hard Mater. 80 (2019) 204–209. https://doi.org/10.1016/j.ijrmhm.2019.01.016.

[24] O.N. Senkov, S. V. Senkova, D.B. Miracle, C. Woodward, Mechanical properties of low-density, refractory multi-principal element alloys of the Cr-Nb-Ti-V-Zr system, Mater. Sci. Eng. A. 565 (2013) 51–62. https://doi.org/10.1016/j.msea.2012.12.018.

[25] J.M. Gregoire, D. Dale, R.B. Van Dover, A wavelet transform algorithm for peak detection and application to powder x-ray diffraction data, Rev. Sci. Instrum. 82 (2011). https://doi.org/10.1063/1.3505103.

[26] D. Gallhofer, B.G. Lottermoser, The influence of spectral interferences on critical element determination with portable X-ray fluorescence (pXRF), Minerals. 8 (2018). https://doi.org/10.3390/min8080320.

[27] C. Wang, W. Ji, Z. Fu, Mechanical alloying and spark plasma sintering of CoCrFeNiMnAl high-entropy alloy, 25 (2014) 1334–1338.

[28] W. Ji, W. Wang, H. Wang, J. Zhang, Y. Wang, F. Zhang, Z. Fu, Alloying behavior and novel properties of CoCrFeNiMn high-entropy alloy fabricated by mechanical alloying and spark plasma sintering, Intermetallics. 56 (2015) 24–27. https://doi.org/10.1016/j.intermet.2014.08.008.

[29] M. Vaidya, A. Karati, A. Marshal, K.G. Pradeep, B.S. Murty, Phase evolution and stability of nanocrystalline CoCrFeNi and CoCrFeMnNi high entropy alloys, J. Alloys Compd. 770 (2019) 1004–1015. https://doi.org/10.1016/j.jallcom.2018.08.200.

[30] Y. Xie, D. Zhou, Y. Luo, T. Xia, W. Zeng, C. Li, J. Wang, J. Liang, D. Zhang, Fabrication of CoCrFeNiMn high entropy alloy matrix composites by thermomechanical consolidation of a mechanically milled powder, Mater. Charact. 148 (2019) 307–316. https://doi.org/10.1016/j.matchar.2019.01.002.

[31] A.J. London, S. Lozano-Perez, S. Santra, S. Amirthapandian, B.K. Panigrahi, C.S. Sundar, C.R.M. Grovenor, Comparison of atom probe tomography and transmission electron microscopy analysis of oxide dispersion strengthened steels, J. Phys. Conf. Ser. 522 (2014). https://doi.org/10.1088/1742-6596/522/1/012028.

[32] M. Laurent-Brocq, P.A. Goujon, J. Monnier, B. Villeroy, L. Perrière, R. Pirès, G. Garcin, Microstructure and mechanical properties of a CoCrFeMnNi high entropy alloy processed by milling and spark plasma sintering, J. Alloys Compd. 780 (2019) 856–865. https://doi.org/10.1016/j.jallcom.2018.11.181.

[33] B. Gwalani, R.M. Pohan, J. Lee, B. Lee, R. Banerjee, H.J. Ryu, S.H. Hong, High-entropy alloy strengthened by in situ formation of entropy-stabilized nano-dispersoids, Sci. Rep. 8 (2018) 1–9. https://doi.org/10.1038/s41598-018-32552-6.

Effect of milling time variation on TiTaVWCr HEA powder as nuclear material on microstructure and mechanical properties by a mechanical alloying method

ORIGINALITY REPORT

0%	0%	0%	0%
SIMILARITY INDEX	INTERNET SOURCES	PUBLICATIONS	STUDENT PAPERS

PRIMARY SOURCES

Exclude quotes	Off	Exclude matches	< 99%
Exclude bibliography	On		